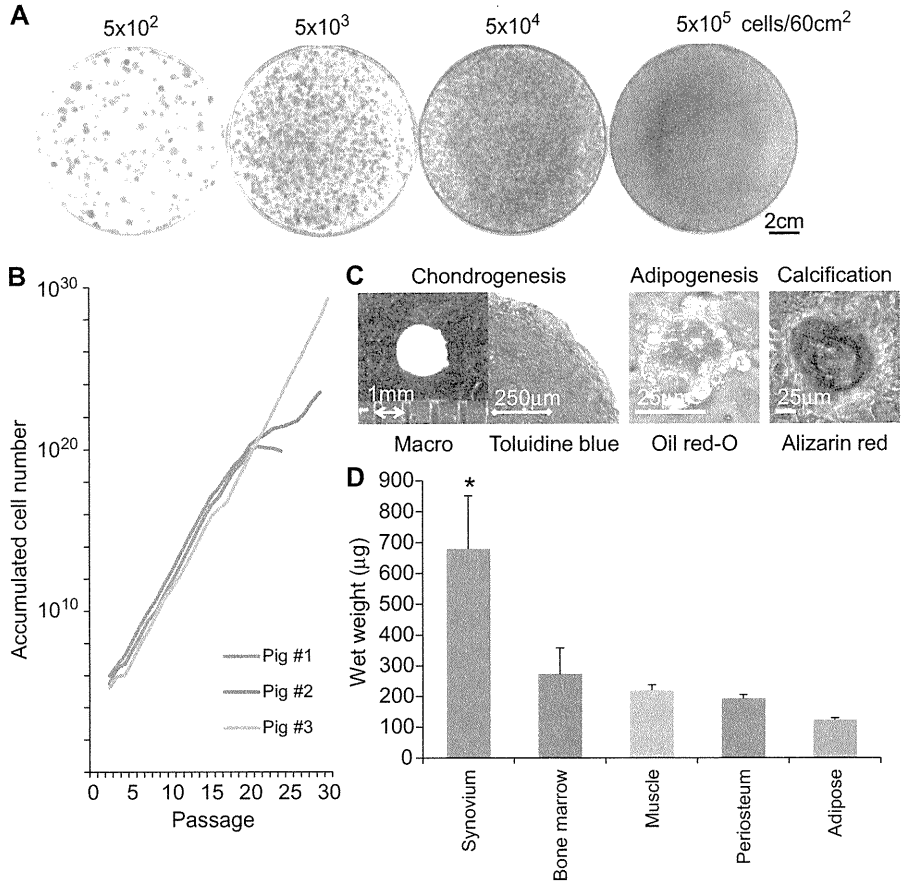

Figure 1. Characteristics of porcine synovial MSCs. (A) Colony formation. (B) Proliferation. (C) *In vitro* chondrogenesis, adipogenesis and calcification. (D) Comparison of the chondrogenic potential among MSCs derived from various mesenchymal tissues. $*P < 0.05$ ($n = 5$) between synovium and each of the other tissues by Wilcoxon rank-sum test.

Arthroscopic and macroscopic observation

At 1 month, a thin membrane covered the cartilage defects only in the *MSC*-treated knees (Figure 3A). At 2 months, a thicker white membrane covered the defects in the *MSC*-treated knees, while the cartilage defects were enlarged in the control knees. At 3 months, the defects were covered with cartilage tissue in the *MSC*-treated knees. In contrast, the defects were further enlarged in the control knees. Arthroscopic observation was easier in the *MSC*-treated knees at all time-points because intra-articular adhesion and synovial hypertrophy were less in the *MSC*-treated knees compared with the control knees. The Oswestry arthroscopy score improved over the course of time, and a significant difference between the two groups was observed at 3 months (Figure 3B). Similar results were obtained with the macroscopic evaluation (Figure 3C). The ICRS score for macroscopic observation was significantly higher in the *MSC*-treated knees than in the control knees (Figure 3D). We found no complications throughout this cell transplantation study in the knees examined.

Histological analyses

At 1 month, membranous tissue completely covered the defects only in the *MSC*-treated knees (Figure 4A). At 3 months, newly synthesized cartilage matrix was observed in every sample in the *MSC*-treated knees. In contrast, there was no cartilage matrix in the control knees (Figure 4B). Furthermore, cartilage defects were further enlarged in the control knees. Higher magnified observations demonstrated a columnar arrangement of chondrocytes with lacunae in the repaired cartilage in the *MSC*-treated knees (Figure 4C, D). The modified Wakitani score for histological analysis of cartilage repair was significantly higher in the *MSC*-treated knees than in the control knees at 3 months (Figure 4E).

dGEMRIC

The cartilage defects showed predominantly red (lower glycosaminoglycan concentration) in both the *MSC* and control knees at 1 month (Figure 5A). At 3 months, they changed to blue (higher glycosaminoglycan concentration) in the *MSC*-treated

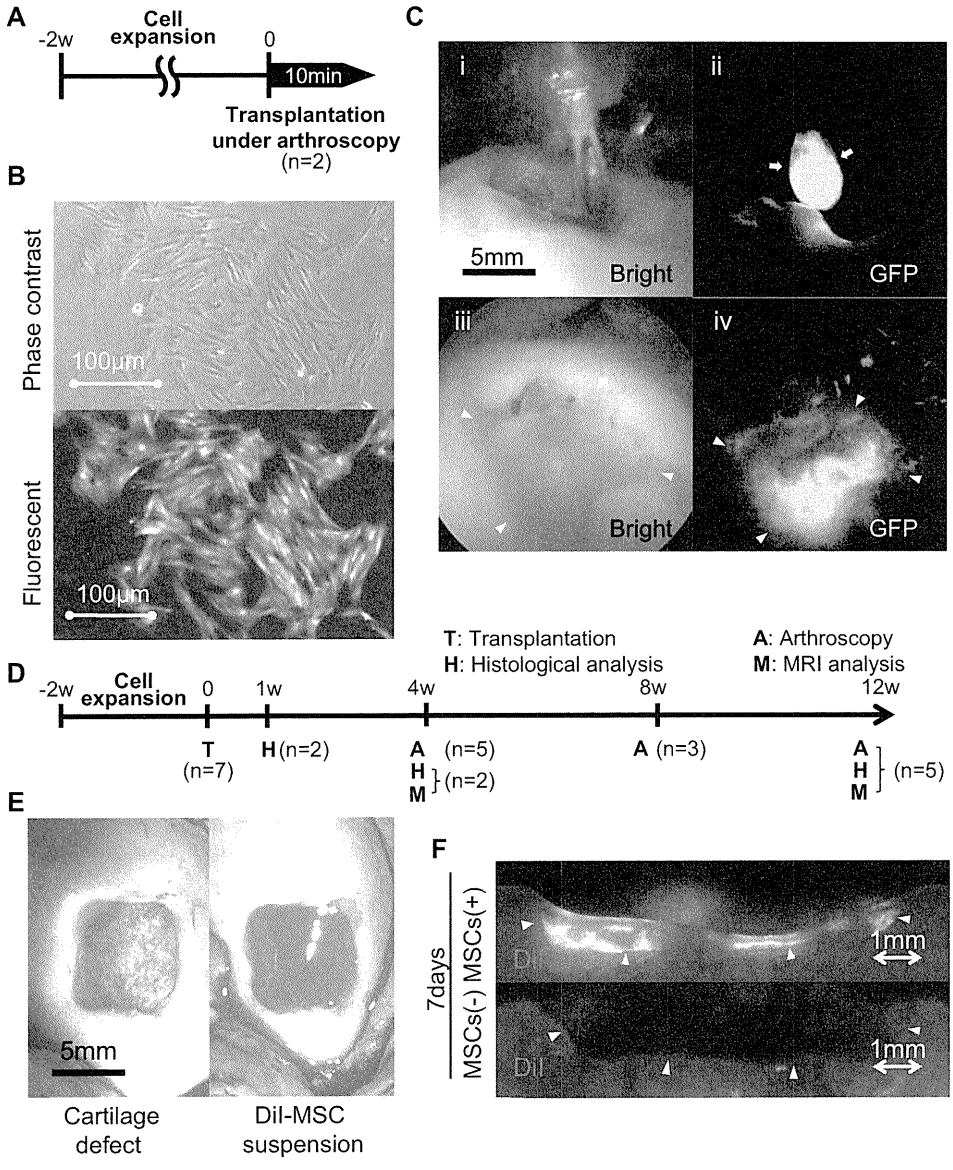

Figure 2. Experimental set-up and local adherent technique for MSCs transplantation. (A) Schematic drawing for arthroscopic transplantation and detection of GFP MSCs. (B) Synovial MSCs from the transgenic GFP pig used to visualize delivery and adhesion of cells in the defect under phase–contrast and fluorescent illumination. (C) Arthroscopic view during transplantation of GFP MSCs into the cartilage defect. Arrows indicate the MSCs suspension leaving the needle. Arrowheads indicate the margin of the cartilage defect. (D) Schematic drawing for histological, MRI and other arthroscopic analyses. (E) Full-thickness cartilage defect (left) and DiI-labeled MSC suspension dropped into the defect (right). (F) Fluorescent images of cartilage defect sections 7 days after transplantation of DiI-labeled MSCs.

knees, while remaining red in the control knees. The average R1 value for ROI (Figure 5B) was higher in the *MSC*-treated knees than in the control knees (Figure 5C).

Discussion

One of the principal findings of the study was the high chondrogenic potential of MSCs from synovium in pigs. In this study, *in vitro* chondrogenesis assays demonstrated that cartilage pellets of MSCs from synovium were heavier than those from bone marrow, muscle, periosteum and adipose tissue in pig. We have reported similar results previously in humans (4), rats (5) and rabbits (22). These findings suggest that MSCs derived from synovium have a high chondrogenic potential irrespective of animal species.

The *in vitro* chondrogenic potential was evaluated by the weight of the pellet. During *in vitro* chondrogenesis of MSCs, the pellets increased in size and weight. In contrast, the DNA yield per pellet decreased over time. The radioactivity per DNA in the cells, assessed by pre-labeling with 3H-thymidine, was stable during *in vitro* chondrogenesis of MSCs. Consequently, the increase in pellet size could be attributed to the production of extracellular matrix (ECM) and not

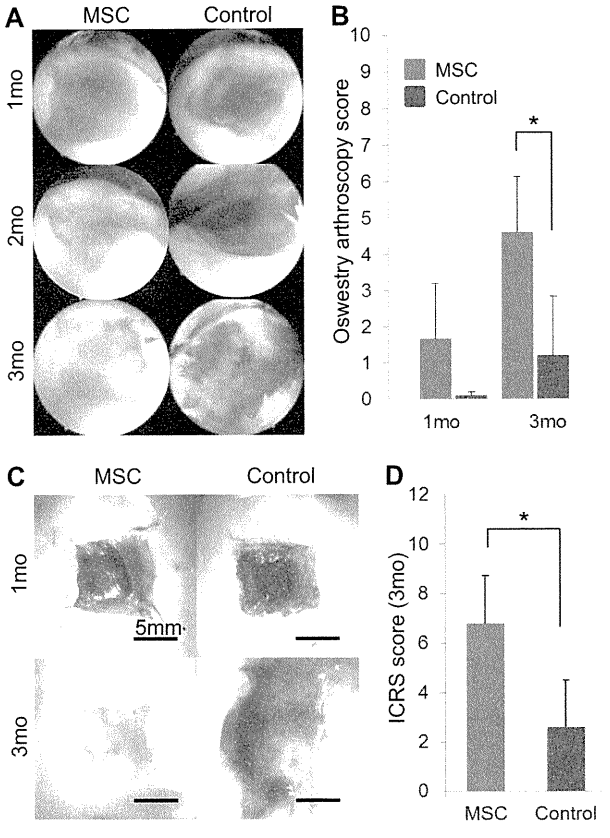

Figure 3. Arthroscopic and macroscopic analyses of cartilage defects with and without transplanted MSC. (A) Sequential arthroscopic view at 1, 2 and 3 months. (B) Quantification of arthroscopic view of cartilage defect. $*P<0.05$ by Wilcoxon rank-sum test. (C) Representative macroscopic features. (D) Quantification of macroscopic features of cartilage defect. $*P<0.05$ by Wilcoxon rank-sum test.

to the proliferation of the cells (19,24). Pellet weight is always correlated with the expression of cartilage-related mRNA, such as COL2A1, with proteoglycan staining by Safranin O, type II collagen by immunostaining, and protein expression of chondroitin 4-sulfate by enzyme-linked immunosorbent assay (ELISA) (4–7,17–19,25). Furthermore, the results of *in vitro* chondrogenesis reflected the results of *in vivo* chondrogenesis in that undifferentiated MSCs were transplanted into cartilage defects, and cartilage matrix production by MSCs was evaluated after 4 weeks in rabbits (6). All the results demonstrate that the weights of the pellets are quantitative indicators for chondrogenesis of MSCs.

In vitro chondrogenesis appears to be most successful when a combination of dexamethasone, TGF-β and BMP is used in MSCs derived from bone marrow (18), synovium (19), muscle (26), periosteum (27) and adipose tissue (28). However, our current results do not exclude the possibility that a different combination of growth factors may induce a more effective chondrogenesis dependent on *MSC* sources.

To track the cells, we used both GFP and DiI systems. The use of GFP cells is advantageous in that dead GFP cells are not detected. In this study, GFP synovial MSCs were derived from the Jinhua pig, and the recipients used were Mexican hairless pigs. This was a major mismatch transplantation model, because Jinhua and Mexican hairless pigs have a high independency of gene profile as a result of inbreeding (29). Therefore, the analysis of transplantation of GFP cells was limited for the observation of arthroscopic transplantation of synovial MSCs, because we wanted to avoid the possibility of an immune reaction after adherence of the cells. The use of GFP cells is disadvantageous in that GFP is often undetectable after processing for histology, especially in the case of paraffin embedding (30). To solve these problems, we used the DiI system to track the transplanted cells.

For histological and other analyses, we created cartilage defects and left the suspension of MSCs on the defects for 10 min in an open arthrotomy. For GFP analysis, after the cartilage defects were created in an open arthrotomy, the joint capsule and skin were sutured, then the suspension of MSCs was placed on the defects through the needle while we observed the defect with an arthroscope, and the suspension was left for 10 min. Fluorescence arthroscopy demonstrated that GFP MSCs remained in the cartilage defects, even though the irrigation fluid was flushed from the tip of the arthroscope. This indicates that the method we used makes it possible to transplant MSCs into the cartilage defects through a small incision by arthroscopy, with minimal invasiveness. Although a GFP-detecting endoscopy system for the airway has been reported previously (31), this system still seems to be unpopular. Our study is the first report demonstrating GFP cells in joints with arthroscopy.

In this study, the number of MSCs adhering to the cartilage defect was not quantified. In our previous *ex vivo* study using human and rabbit samples, a suspension of synovial MSCs was placed on the full-thickness defect of the articular cartilage fragment, and approximately 60% of the cells were attached to the defect within 10 min (11). A recent study reported that the addition of magnesium to the cell suspension increased the number of synovial MSCs attached to the cartilage defect *in vitro* and *in vivo* (32). In our pig study, the medium for *MSC* suspension contained 1 mM magnesium, and we estimated that more than 60% of the cells adhered to the cartilage defect.

The cartilage defect we created might be better called an osteochondral defect rather than a cartilage defect. We tried to create a full thickness cartilage

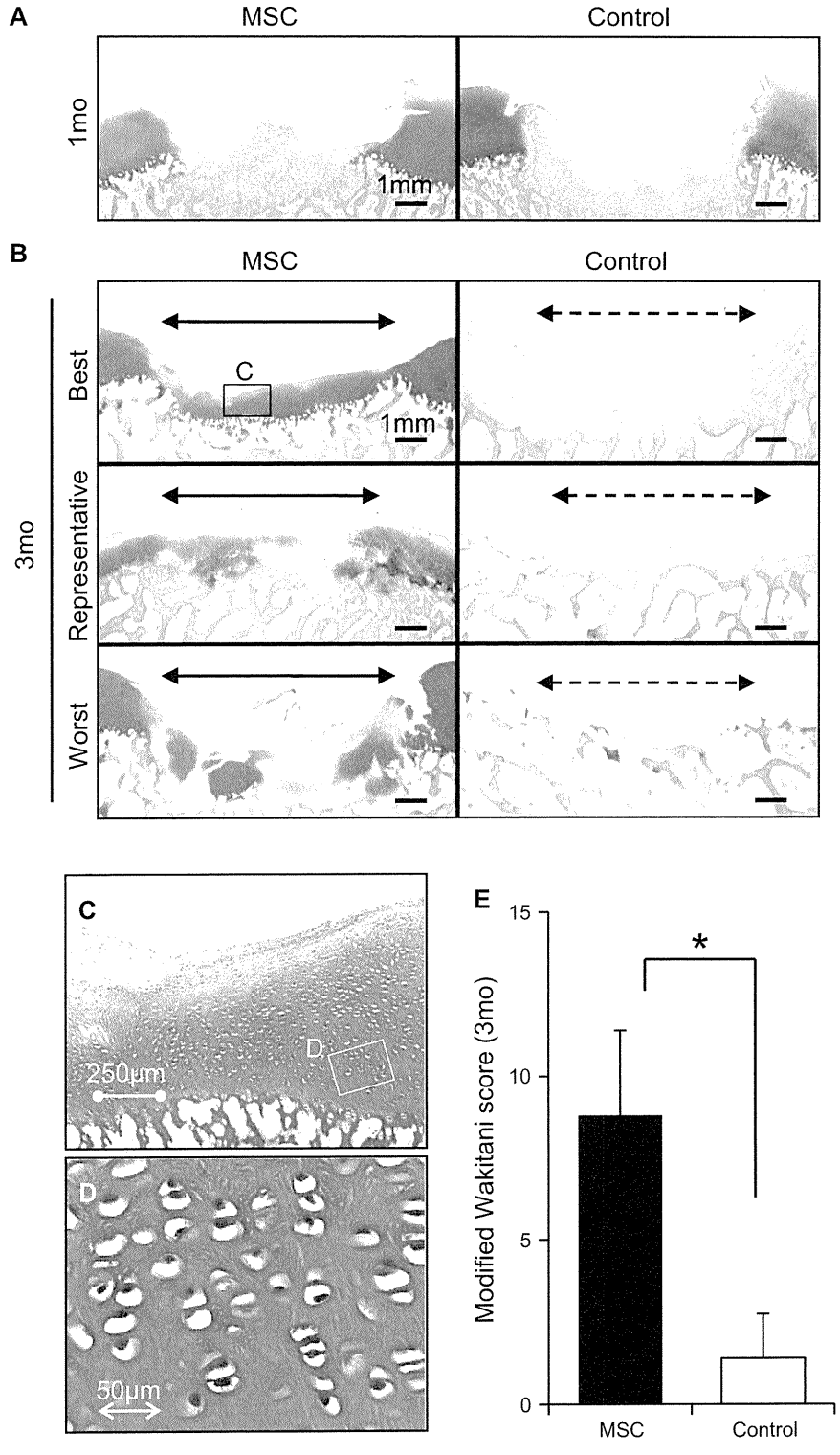

Figure 4. Histological analyses of cartilage defect transplanted with MSCs. (A) Representative sections stained with Safranin O at 1 month. Red indicates extracellular matrix, and blue indicates cancellous bone. (B) Example sections of the best, representative and worst outcomes in the MSC-treated knees at 3 months and in the control from the opposite sides. Borders of the original defect are shown by both arrowheads. (C) Magnified histology of the indicated area. (D) High magnification of the indicated area. (E) Quantification of histologies of cartilage defect. $*P < 0.05$ by Wilcoxon rank-sum test.

defect, but it was not technically easy to do with precision. Therefore, we preferred to create the osteochondral defect in order to be sure all the cartilage was removed, because any remaining cartilage would affect the outcome of this study. We also thought that if we could repair an osteochondral defect with our

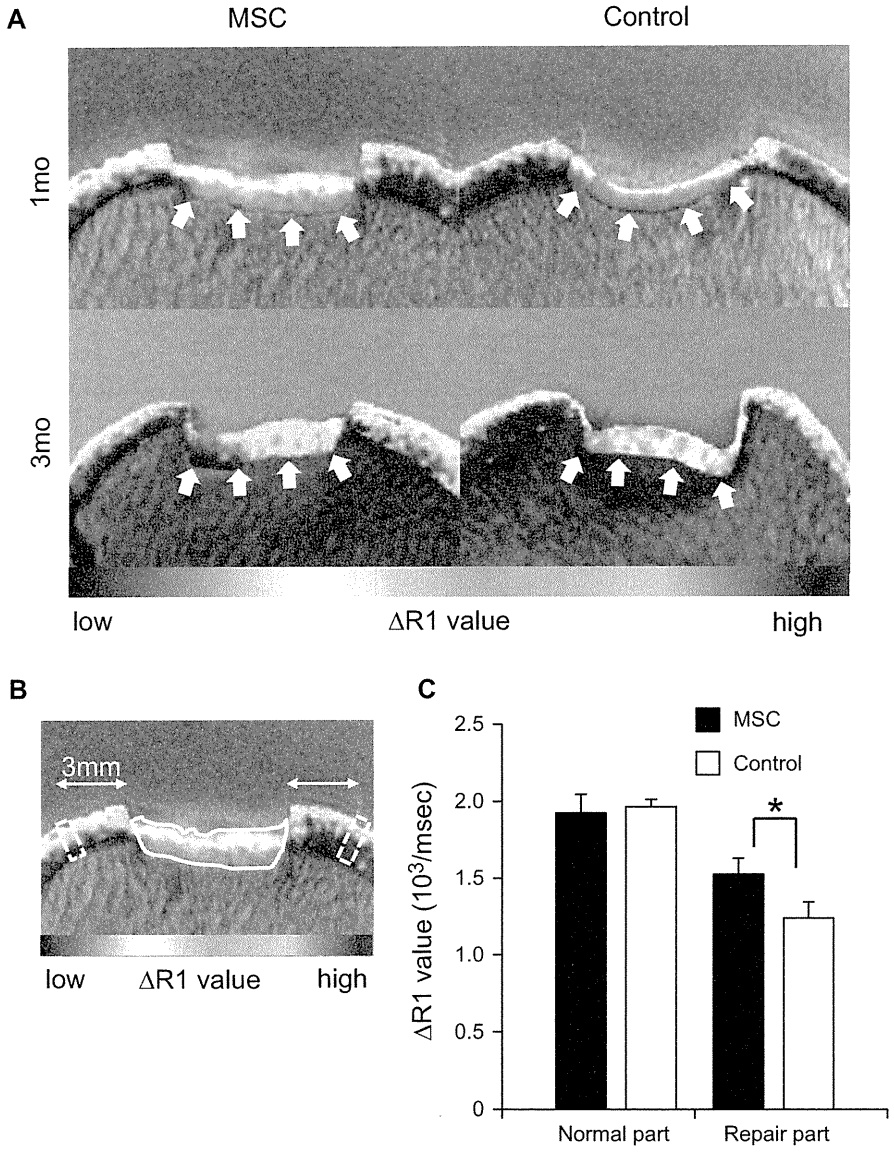

Figure 5. Evaluation with dGEMRIC. (A) Representative images. Arrows indicate the bottoms of the repair tissue. (B) ROI for repaired cartilage (solid-line area) and for native cartilage (dotted-line areas). (C) Quantification of R1 values at 3 months. $*P<0.05$ by paired t-test.

method, we could also repair a full thickness cartilage defect through further abrading of the full thickness cartilage defect to create an osteochondral defect.

By penetrating the subchondral bone, host bone marrow MSCs would have migrated into the defect. Because bone marrow MSCs also have chondrogenic potential (33), the effect of bone marrow MSCs would not have been negligible in our study. However, we were able to demonstrate the higher effect of synovial MSCs, because the control defects were not repaired at all. The depth of the osteochondral defect may have affected the result of the repair. Chang *et al.* (34) compared the histological score of the spontaneous repair of the defect between a 2-mm and 5-mm depth of osteochondral defect in pigs for 36 weeks, and the score of the 2-mm defect was better than that of the 5-mm osteochondral defect. In our study, a 2-mm osteochondral defect consisting of 1.5 mm in the cartilage and 0.5 mm in the subchondral bone was created, and the influence of the subchondral bone defect would have been less than that when the subchondral bone was penetrated deeper.

In this study, DiI-labeled cells were detected at 1 week, but not at 4 and 12 weeks. The process of cartilage repair was observed within at least 3 months. These findings suggest that transplantation of synovial MSCs secretes some trophic factors to enhance cartilage repair rather than directly differentiating into chondrocytes. According to our recent report, in a co-culture of rat nucleus pulposus cells and human synovial MSCs, a species-specific microarray revealed that gene profiles of the nucleus pulposus were altered markedly, with suppression of genes related to matrix degradative enzymes and inflammatory cytokines (35).

Identification of the trophic factors by synovial MSCs in a cartilage defect model is required in a future study.

We have shown that transplantation of synovial MSCs into cartilage defect promotes cartilage repair in pigs. To the best of our knowledge, only Ando *et al.* (36) have previously reported the effect of transplantation of synovial MSCs into cartilage defects in a pig model. They cultured synovial MSCs at a high density in growth medium containing ascorbate 2-phosphate, to form a complex of the cultured cells and the extracellular matrix. After detaching the tissue-engineered construct by application of shear stress using gentle pipetting, the constructs were implanted into the cartilage defect (36). Comparing Ando *et al.*'s study (36) and ours, our method is simpler, and we provide several kinds of novel information during the process of cartilage repair.

We have reported previously that placing a synovial *MSC* suspension on the osteochondral defect for 10 min promotes cartilage regeneration in rabbits. Histological analyses demonstrated that the osteochondral defect was initially filled with cartilage matrix at 4 weeks, then the border between the bone and cartilage moved upward, and finally the thickness of the regenerated cartilage became similar to that of the neighboring cartilage in rabbits (11,32). In the pig study, after transplantation of synovial MSCs, the cartilage defect was first covered with a membrane at 4 weeks, then the cartilage matrix emerged, although the repair of the subchondral bone was not observed. These findings may indicate different processes of cartilage repair between rabbits and pigs.

After placement of the *MSC* suspension, consisting of on average 38 million cells in 100 μL, for 10 min, although the inside of the knee joint was filled with irrigation fluid flushed from the tip of the arthroscope, the bottom of the cartilage defect looked foggy through conventional light arthroscopy (Figure 2Ciii). This was possible because the cartilage defect was mostly covered with synovial MSCs. The color of the suspension of synovial MSCs was similar to that of the cartilage defect after placement of the *MSC* suspension for 10 min, which supports our speculation. For clinical application, we can guess the existence of MSCs without labeling, by arthroscopic observation if a high concentration of *MSC* suspension is prepared.

dGEMRIC requires more effort than conventional MRI because it requires twice as many imagings both before and after contrast agent administration. However, dGEMRIC can provide information about the thickness of repaired cartilage and glycosaminoglycan concentration (14,15). In this study, we confirmed the usefulness of dGEMRIC for cartilage repair. To the best of our knowledge, this is the first study to analyze porcine cartilage repair by dGEMRIC and to compare its histological results.

Although transplantation of synovial MSCs induced cartilage repair compared with control knees, cartilage repair was not yet complete at 3 months. We can suggest three reasons for this. First, 3 months was too short a time to mature the cartilage defect in this model. Even in our rabbit study, it took 6 months to repair the cartilage defect after transplantation of synovial MSCs (22). In porcine studies by others, it seems that cartilage repair was not complete at 6 months after bone marrow MSCs transplantation (37–39). Because of the limitation of our animal facility, we could not perform observations for more than 3 months in this study. Second, we created the cartilage defect in both knees, and all pigs were free in the cage. Therefore, both knees could not avoid bearing weight. Third, allogeneic synovial MSCs were used in this study to prevent variability of porcine MSCs.

However, this study is valuable because we have demonstrated the ability of synovial-derived MSCs to repair cartilage in the porcine knee relative to vehicle-treated knees. Furthermore, the potential problems in this study, as mentioned above, can be overcome if and when this therapy is applied in humans, because weight bearing can be controlled on the treated knee, and autologous cells can be prepared to expand in autologous human serum (7).

In conclusion, an *in vitro* chondrogenesis assay revealed that MSCs from synovium had a higher chondrogenic potential than that from other mesenchymal tissues in pig, as has been found in other species (4,5,22). Through the use of transgenic porcine GFP-expressing synovial MSCs and a new fluorescence arthroscopy system, we were able to visualize the actual delivery and adhesion of the cells in the cartilage defect. We utilized dGEMRIC to obtain detailed serial images of cartilage repair produced by MSCs. Sequential arthroscopic, histological and MRI analyses demonstrated that the cartilage defect was first covered with a membrane, and then the cartilage matrix emerged after transplantation of synovial MSCs (Figure 6).

Acknowledgments

We thank Miyoko Ojima for her expert help with histology, Izumi Nakagawa for her management of our laboratory, and Toru Wakui, Minoru Yamada and Yoko Sekiyama in the pig center of Jichi Medical University for their expert support with preparing experiments and animal care.

This study was supported by "the Project for Realization of Regenerative Medicine" by the Ministry of Education, Culture, Sports, Science and

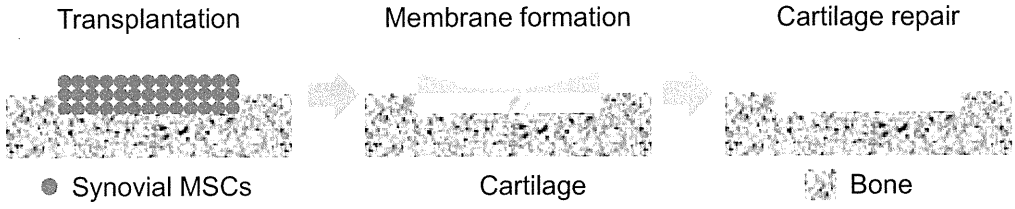

Figure 6. Diagram of the process of cartilage repair. At about 1 month, a membranous layer formed over the defect, and by 3 months cartilage had formed to repair the defect.

Technology (MEXT), Japan, and by "the Japanese Foundation for Research and Promotion of Endoscopy" to IS, by "the Global Center of Excellence (GCOE) Program" by MEXT to TM, and by "the Strategic Research Platform for Private Universities: Matching Fund Subsidy" by MEXT to EK.

Author contributions: TN, IS, TM and EK designed the experiments; TN and IS wrote the manuscript; TN performed experiments and collected and analyzed data; IS, TM and EK supervised the project and provided study materials and financial support; DH and MH assisted with the porcine experiment; KT proofread the manuscript; TK provided the GFP transgenic pig; AW performed magnetic resonance imaging, and analyzed data; SH, YF and HT provided and managed the pigs.

Disclosure of interests: The authors declare no competing interests.

References

1. Mankin HJ. The response of articular cartilage to mechanical injury. J Bone Joint Surg Am. 1982;64:460–6.
2. Chen F, Rousche K, Tuan R. Technology insight: adult stem cells in cartilage regeneration and tissue engineering. Nat Clin Pract Rheumatol. 2006;2:373–82.
3. Koga H, Engebretsen L, Brinchmann J, Muneta T, Sekiya I. Mesenchymal stem cell-based therapy for cartilage repair: a review. Knee Surg Sports Traumatol Arthrosc. 2009;17:1289–97.
4. Sakaguchi Y, Sekiya I, Yagishita K, Muneta T. Comparison of human stem cells derived from various mesenchymal tissues: superiority of synovium as a cell source. Arthritis Rheum. 2005;52:2521–9.
5. Yoshimura H, Muneta T, Nimura A, Yokoyama A, Koga H, Sekiya I. Comparison of rat mesenchymal stem cells derived from bone marrow, synovium, periosteum, adipose tissue, and muscle. Cell Tissue Res. 2007;327:449–62.
6. Koga H, Muneta T, Nagase T, Nimura A, Ju Y, Mochizuki T, et al. Comparison of mesenchymal tissue-derived stem cells for in vivo chondrogenesis: suitable conditions for cell therapy of cartilage defects in rabbit. Cell Tissue Res. 2008;333: 207–15.
7. Nimura A, Muneta T, Koga H, Mochizuki T, Suzuki K, Makino H, et al. Increased proliferation of human synovial mesenchymal stem cells with autologous human serum: comparisons with bone marrow mesenchymal stem cells and with fetal bovine serum. Arthritis Rheum. 2008;58:501–10.
8. Murphy J, Fink D, Hunziker E, Barry F. Stem cell therapy in a caprine model of osteoarthritis. Arthritis Rheum. 2003;48: 3464–74.
9. Lee K, Hui J, Song I, Ardany L, Lee E. Injectable mesenchymal stem cell therapy for large cartilage defects: a porcine model. Stem Cells. 2007;25:2964–71.
10. Wakitani S, Imoto K, Yamamoto T, Saito M, Murata N, Yoneda M. Human autologous culture expanded bone marrow mesenchymal cell transplantation for repair of cartilage defects in osteoarthritic knees. Osteoarthritis Cartilage. 2002; 10:199–206.
11. Koga H, Shimaya M, Muneta T, Nimura A, Morito T, Hayashi M, et al. Local adherent technique for transplanting mesenchymal stem cells as a potential treatment of cartilage defect. Arthritis Res Ther. 2008;10:R84.
12. Chu C, Szczodry M, Bruno S. Animal models for cartilage regeneration and repair. Tissue Eng Part B Rev. 2010;16:105–15.
13. Schulze-Tanzil G, Müller R, Kohl B, Schneider N, Ertel W, Ipaktchi K, et al. Differing in vitro biology of equine, ovine, porcine and human articular chondrocytes derived from the knee joint: an immunomorphological study. Histochem Cell Biol. 2009;131:219–29.
14. Watanabe A, Wada Y, Obata T, Ueda T, Tamura M, Ikehira H, et al. Delayed gadolinium-enhanced MR to determine glycosaminoglycan concentration in reparative cartilage after autologous chondrocyte implantation: preliminary results. Radiology. 2006;239:201–8.
15. Watanabe A, Obata T, Ikehira H, Ueda T, Moriya H, Wada Y. Degeneration of patellar cartilage in patients with recurrent patellar dislocation following conservative treatment: evaluation with delayed gadolinium-enhanced magnetic resonance imaging of cartilage. Osteoarthritis Cartilage. 2009;17:1546–53.
16. Kawarasaki T, Uchiyama K, Hirao A, Azuma S, Otake M, Shibata M, et al. Profile of new green fluorescent protein transgenic Jinhua pigs as an imaging source. J Biomed Opt. 2009;14:054017.
17. Sekiya I, Colter D, Prockop D. BMP-6 enhances chondrogenesis in a subpopulation of human marrow stromal cells. Biochem Biophys Res Commun. 2001;284:411–8.
18. Sekiya I, Larson B, Vuoristo J, Reger R, Prockop D. Comparison of effect of BMP-2, -4, and -6 on in vitro cartilage formation of human adult stem cells from bone marrow stroma. Cell Tissue Res. 2005;320:269–76.
19. Shirasawa S, Sekiya I, Sakaguchi Y, Yagishita K, Ichinose S, Muneta T. In vitro chondrogenesis of human synovium-derived mesenchymal stem cells: optimal condition and comparison with bone marrow-derived cells. J Cell Biochem. 2006;97:84–97.
20. Sekiya I, Larson B, Vuoristo J, Cui J, Prockop D. Adipogenic differentiation of human adult stem cells from bone marrow stroma (MSCs). J Bone Miner Res. 2004;19:256–64.
21. Sekiya I, Larson B, Smith J, Pochampally R, Cui J, Prockop D. Expansion of human adult stem cells from bone marrow stroma: conditions that maximize the yields of early progenitors and evaluate their quality. Stem Cells. 2002;20:530–41.
22. Koga H, Muneta T, Ju Y, Nagase T, Nimura A, Mochizuki T, et al. Synovial stem cells are regionally specified according to local microenvironments after implantation for cartilage regeneration. Stem Cells. 2007;25:689–96.

23. van den Borne M, Raijmakers N, Vanlauwe J, Victor J, de Jong S, Bellemans J, et al. International Cartilage Repair Society (ICRS) and Oswestry macroscopic cartilage evaluation scores validated for use in autologous chondrocyte implantation (ACI) and microfracture. Osteoarth Cart. 2007;15:1397–402.
24. Sekiya I, Vuoristo J, Larson B, Prockop D. In vitro cartilage formation by human adult stem cells from bone marrow stroma defines the sequence of cellular and molecular events during chondrogenesis. Proc Natl Acad Sci USA. 2002;99: 4397–402.
25. Mochizuki T, Muneta T, Sakaguchi Y, Nimura A, Yokoyama A, Koga H, et al. Higher chondrogenic potential of fibrous synovium- and adipose synovium-derived cells compared with subcutaneous fat-derived cells: distinguishing properties of mesenchymal stem cells in humans. Arthritis Rheum. 2006;54: 843–53.
26. Kuroda R, Usas A, Kubo S, Corsi K, Peng H, Rose T, et al. Cartilage repair using bone morphogenetic protein 4 and muscle-derived stem cells. Arthritis Rheum. 2006;54:433–42.
27. Ringe J, Leinhase I, Stich S, Loch A, Neumann K, Haisch A, et al. Human mastoid periosteum-derived stem cells: promising candidates for skeletal tissue engineering. J Tissue Eng Regen Med. 2008;2:136–46.
28. Puetzer J, Petitte J, Loboa E. Comparative review of growth factors for induction of three-dimensional in vitro chondrogenesis in human mesenchymal stem cells isolated from bone marrow and adipose tissue. Tissue Eng Part B Rev. 2010;16: 435–44.
29. Li SJ, Yang SL, Yang SH, Zhao SH, Fan B, Yu M, et al. Genetic diversity analyses of 10 indigenous Chinese pig populations based on 20 microsatellites. J Anim Sci. 2004;82: 368–74.
30. Ikawa M, Kominami K, Yoshimura Y, Tanaka K, Nishimune Y, Okabe M. Green fluorescent protein as a marker in transgenic mice. Devel Growth Diff. 1995;37: 455–9.
31. Flotte TR, Beck SE, Chesnut K, Potter M, Poirier A, Zolotukhin S. A fluorescence video-endoscopy technique for detection of gene transfer and expression. Gene Ther. 1998;5: 166–73.
32. Shimaya M, Muneta T, Ichinose S, Tsuji K, Sekiya I. Magnesium enhances adherence and cartilage formation of synovial mesenchymal stem cells through integrins. Osteoarth Cart. 2010;18: 1300–9.
33. Wakitani S, Goto T, Pineda S, Young R, Mansour J, Caplan A, et al. Mesenchymal cell-based repair of large, full-thickness defects of articular cartilage. J Bone Joint Surg Am. 1994;76: 579–92.
34. Chang CH, Kuo TF, Lin CC, Chou CH, Chen KH, Lin FH, et al. Tissue engineering-based cartilage repair with allogenous chondrocytes and gelatin-chondroitin-hyaluronan tricopolymer scaffold: a porcine model assessed at 18, 24, and 36 weeks. Biomaterials. 2006;27:1876–88.
35. Miyamoto T, Muneta T, Tabuchi T, Matsumoto K, Saito H, Tsuji K, et al. Intradiscal transplantation of synovial mesenchymal stem cells prevents intervertebral disc degeneration through suppression of matrix metalloproteinase-related genes in nucleus pulposus cells in rabbits. Arthritis Res Ther. 2010;12:R206.
36. Ando W, Tateishi K, Hart D, Katakai D, Tanaka Y, Nakata K, et al. Cartilage repair using an in vitro generated scaffold-free tissue-engineered construct derived from porcine synovial mesenchymal stem cells. Biomaterials. 2007;28:5462–70.
37. Zhou G, Liu W, Cui L, Wang X, Liu T, Cao Y. Repair of porcine articular osteochondral defects in non-weightbearing areas with autologous bone marrow stromal cells. Tissue Eng. 2006;12:3209–21.
38. Chiang H, Kuo T, Tsai C, Lin M, She B, Huang Y, et al. Repair of porcine articular cartilage defect with autologous chondrocyte transplantation. J Orthop Res. 2005;23:584–93.
39. Jiang C, Chiang H, Liao C, Lin Y, Kuo T, Shieh C, et al. Repair of porcine articular cartilage defect with a biphasic osteochondral composite. J Orthop Res. 2007;25:1277–90.

Supplementary material available online

Supplementary Movies I–II.
Supplementary Tables I–III.

Cell Medicine, Vol. 4, pp. 13–21, 2012
Printed in the USA.

2155-1790/12 $90.00 + .00
DOI: http://dx.doi.org/10.3727/215517912X653319
www.cognizantcommunication.com

Comparison of Gingiva, Dental Pulp, and Periodontal Ligament Cells From the Standpoint of Mesenchymal Stem Cell Properties

Koji Otabe,* Takeshi Muneta,*† Nobuyuki Kawashima,‡ Hideaki Suda,†‡
Kunikazu Tsuji,† and Ichiro Sekiya§

*Orthopedic Surgery, Graduate School of Medical and Dental Sciences, Tokyo Medical and Dental University, Tokyo, Japan
†Global Center of Excellence Program for International Research Center for Molecular Science in Tooth and Bone Disease, Tokyo Medical and Dental University, Tokyo, Japan
‡Pulp Biology and Endodontics, Graduate School of Medical and Dental Sciences, Tokyo Medical and Dental University, Tokyo, Japan
§Cartilage Regeneration, Graduate School of Medical and Dental Sciences, Tokyo Medical and Dental University, Tokyo, Japan

The specific properties of mesenchymal stem cells (MSCs) in oral tissues still remain unknown though their existence has been previously reported. We collected gingiva, dental pulp, and periodontal ligament tissues from removed teeth and isolated MSCs. These MSCs were compared in terms of their yields per tooth, surface epitopes, and differentiation potentials by patient-matched analysis. For in vivo calcification analysis, rat gingival and dental pulp cells mounted on β-tricalcium phospateTCP were transplanted into the perivertebral muscle of rats for 6 weeks. Gingival cells and dental pulp cells showed higher yield per tooth than periodontal ligament cells ($n=6$, $p<0.05$). Yields of periodontal ligament cells were too low for further analysis. Gingival and dental pulp cells expressed MSC markers such as CD44, CD90, and CD166. Gingival and dental pulp cells obtained phenotypes of chondrocytes and adipocytes in vitro. Approximately 60% of the colonies of gingival cells and 40% of the colonies of dental pulp cells were positively stained with alizarin red in vitro, and both gingival and dental pulp cells were calcified in vivo. We clarified properties of MSCs derived from removed teeth. We could obtain a high yield of MSCs with osteogenic potential from gingiva and dental pulp. These results indicate that gingiva and dental pulp are putative cell sources for hard tissue regeneration.

Key words: Mesenchymal stem cells (MSCs); Gingiva; Dental pulp; Periodontal ligament; Yields; Differentiation

INTRODUCTION

Mesenchymal stem cells (MSCs) are a heterogeneous population and are defined as being derived from mesenchymal tissue and by their functional capacity to form colonies and to differentiate into bone, cartilage, and adipose cells in vitro (23). These cells participate in tissue homeostasis, remodeling, and repair by ensuring replacement of mature cells that are lost during the course of physiological turnover, injury, or disease (2). MSCs can be isolated from various mesenchymal tissues, and MSCs contain common features independent of their origin, but an increasing number of reports describe their distinguishing properties dependent on origin.

MSCs can be obtained from oral tissues such as gingiva (21,25), dental pulp (1,4,12), and periodontal ligament (1,5,11,17,22). These tissues can be obtained from a removed tooth and are useful for regenerative medicine if they are efficient cell sources for MSCs. However, the optimal cell source for MSCs in a removed tooth remains unknown because gingival, dental pulp, and periodontal ligament cells have not been compared from the standpoint of the properties of MSCs.

In this study, we collected gingiva, dental pulp, and periodontal ligament from removed teeth and isolated MSCs with the same method. MSCs derived from gingiva, dental pulp, and periodontal ligament were compared in terms of their yields per tooth, surface epitopes,

Received January 26, 2012; June 6, 2012. Online prepub date: August 10, 2012.
Address correspondence correspondence to Ichiro Sekiya M.D., Ph.D., Section of Cartilage Regeneration, Graduate School, Tokyo Medical and Dental University, 1-5-45 Yushima, Bunkyo-ku, Tokyo, 113-8519, Japan. Tel: +81-3-5803-4675; Fax: +81-3-5803-0266; E-mail: sekiya.orj@tmd.ac.jp

and differentiation potentials. Our results demonstrate the optimal cell source of MSCs in the removed tooth and indicate one possible application for regeneration therapy.

MATERIALS AND METHODS

Tissue Harvest and Cell Preparation

This study was approved by our institutional review board, and informed consent was obtained from all patients. Twelve human healthy impacted third molars, removed by orthodontic treatment, were used for this study. The age of the subjects ranged between 20 and 40 years. Gingiva, dental pulp, and periodontal ligament were collected from the removed molars. As Somerman et al. reported previously, the remaining gingival tissues from the cervical area of the root surface were curetted away with care to avoid contamination of the periodontal ligament tissues by gingival connective tissues. Furthermore, periodontal ligament tissues attached to the middle third of the root were mainly curetted and corrected to reduce contamination with both gingival and apical tissue (19). The corrected tissues were minced by scalpel, washed in 1 ml of phosphate-buffered saline (PBS) containing 100 units/ml penicillin amphotericin B (Invitrogen) three times to prevent oral normal bacterial and fungal contamination, and then digested with 3 mg/ml of type 5 collagenase (Sigma-Aldrich, St. Louis, MO) in αMEM (α-modified Eagle's medium; Invitrogen) for 2 h at 37°C. Then, the cells were passed through a 70-μm nylon filter (Becton Dickinson Bioscience, Bedford, MA) to remove undigested debris, counted with a hemocytometer, and cultured in a complete culture medium [αMEM containing 10% fetal bovine serum (Invitrogen), 100 units/ml penicillin, 100 μg/ml streptomycin, and 250 ng/ml amphotericin B)] at a density of 1×10^3, 1×10^4, 1×10^5 cells/60 cm^2 dish (Nalge Nunc International, Rochester, NY) for 14 days. Three dishes were stained with 0.5% crystal violet, and colonies larger than 2 mm in diameter were counted. The optimal initial cell density was determined based on the following criteria: 1) the colony size was not affected by colony-to-colony contact inhibition and 2) the largest number of colonies was obtained. The cells were harvested with 0.25% trypsin and 1 mm Ethylenediaminetetraacetic acid [EDTA, (Invitrogen)] at 37°C for 5 min and were then counted with a hemocytometer to determine the total yields of cells per tooth at passage 0. The cells were replated, cultured, and harvested with trypsin-EDTA every 14 days at optimal initial cell density, and passage 2 cells were used for further analysis.

Surface Epitopes

Two million passage 2 cells were suspended in 1 ml PBS with antibodies, incubated for 30 min at 4°C, then resuspended in 1 ml of PBS. Fluorescein isothiocyanate (FITC)-, or phycoerythrin (PE)-, coupled antibodies against cluster of differentiation 34 (CD34), CD45, CD90 and CD146 were from Becton Dickinson (Franklin Lakes, NJ); CD44 and CD117 were from eBioscience (San Diego, CA); CD105 and CD166 were from Ancell Corporation (Bayport, MN). For the isotype control, FITC- or PE-coupled nonspecific mouse IgG (Becton Dickinson) was substituted for the primary antibody. Cell fluorescence was evaluated by FACSCalibur instrument (Becton Dickinson), and data were analyzed using CellQuest software (Becton Dickinson).

Synovial MSCs

Human synovium was harvested from three male donors (20, 23, and 30 years old) during an operation for anterior cruciate ligament reconstruction of the knee. The synovium was minced and digested with 3 mg/ml collagenase for 3 h, and then the tissues were filtered with a 70-μm nylon filter. The nucleated cells were plated at 1×10^4 cells/60 cm^2 dish, cultured for 14 days, and replated at 1×10^5 cells/150 cm^2 dish. The cells were cultured every 14 days, and passage 2 cells were used for further analysis (15).

Chondrogenesis

Passage 2 cells (2.5×10^5) were placed in a 15-ml polypropylene tube (Falcon, Bedford, MA) and pelleted by centrifugation at 450×*g* for 10 min. The pellets were cultured for 21 days in chondrogenic media, which contained 1000 ng/ml bone morphogenetic protein 7 (BMP-7; Stryker Biotech, Hopkinton, MA), in addition to high-glucose Dulbecco's modified Eagle's medium (Invitrogen) supplemented with 10 ng/ml transforming growth factor (TGF)-β3 (R&D Systems, Minneapolis, MN), 100 nM dexamethasone (Wako, Tokyo, Japan), ascorbate-2-phosphate (Sigma-Aldrich), L-proline (Sigma-Aldrich), pyruvate (Sigma-Aldrich), and insulin–transferrin–selenium premix (Becton Dickinson) (15).

For type 2 collagen immunostain, sections were deparaffinized, washed in PBS, and then pretreated with 0.4 mg/ml proteinase K (DAKO, Carpinteria, CA) in Tris–HCl buffer for 15 min at room temperature for antigen retrieval. The tissue sections were incubated with mouse monoclonal anti-human type 2 collagen antibody (1:200 dilution; Daiichi Fine Chemical, Toyama, Japan) for 1 h at room temperature. After extensive washes with PBS, the sections were incubated with biotinylated horse anti-mouse IgG secondary antibody (Vector Laboratories) for 30 min at room temperature. Immunostaining was detected with the Vectastain ABC reagent (Vector Laboratories) followed by diaminobenzidine staining.

Adipogenesis

One hundred passage 2 cells were plated in 60-cm^2 dishes and cultured in complete medium for 14 days.

Then the medium was switched to adipogenic medium, which consisted of complete medium supplemented with 10^{-7} M dexamethasone, 0.5 mm isobutyl-1-methyl xanthine (Sigma-Aldrich), and 100 μm indomethacin (Wako) for 21 days. The cells were fixed in 4% paraformaldehyde and stained with fresh oil red O solution (Sigma-Aldrich). After taking pictures of the dishes, they were overstained with crystal violet (13).

Osteogenesis In Vitro

One hundred passage 2 cells were plated in 150-cm^2 dishes and cultured in complete medium for 14 days. Then the medium was switched to osteogenic medium, which consisted of complete medium supplemented with 1 nM dexamethasone, 10 mM β-glycerol phosphate (Wako), and 50 μg/ml ascorbate-2-phosphates for 21 days. The dishes were stained with 0.5% alizarin red solution (Sigma-Aldrich). After taking pictures of the dishes, they were overstained with crystal violet (13).

Quantitative PCR

For chondrogenesis, 2.5×10^5 cells were pelleted and cultured in chondrogenic medium for 21 days. Undifferentiated 2×10^6 cells and eight pellets were used for RNA collection. For adipogenesis and osteogenesis, undifferentiated 1×10^5 cells were initially plated on a 60-cm^2 dish and cultured in complete medium for 14 days. Then the medium was switched to adipogenic and osteogenic medium, and the cells were cultured for 21 days. Four dishes before and after the inductions were used for RNA collection. Total RNA was prepared by using TRIzol Reagent (Invitrogen). Pellets were homogenized before preparation. Total RNA was purified by RNeasy Mini kit (QIAGEN, Valencia, CA). One microgram of total RNA was reverse transcribed into first-strand cDNA with a Transcriptor High Fidelity cDNA Synthesis Kit (Roche Diagnostics, Manheim, Germany).

Quantitative plymerase chain reaction (PCR) analysis was conducted on a LightCycler® 480 Real-Time PCR System (Roche Diagnostics) using a FastStart TaqMan® Probe Master Kit (Roche Diagnostics) for 45 cycles with denaturation at 95°C for 15 s and annealing at 60°C for 60 s. Each procedure was repeated three times. The amounts of mRNA were calculated as relative quantities in comparison to that of β-actin mRNA. PCR primers were as follows:

Aggrecan:	5′-CCTCCCCTTCACGTGTAAAA-3′ (forward), 5′-GCTCCGCTTCTGTAGTCTGC-3′ (reverse);
Adipsin:	5′-TCCAAGCGCCTGTACGAC-3′ (forward), 5′-GTGTGGCCTTCTCCGACA-3′ (reverse);
Runx2:	5′-CACCATGTCAGCAAAACTTCTT-3′ (forward), 5′-TCACGTCGCTCATTTTGC-3′ (reverse);
Osteocalcin:	5′-TGAGAGCCCTCACACTCCTC-3′ (forward), 5′-CCTCCTGCTTGGACACAAAG-3′ (reverse);
β-actin:	5′-ATTGGCAATGAGCGGTTC-3′ (forward), 5′-TGAAGGTAGTTTCGTGGATGC-3′ (reverse).

Runx2, Runt-related transcription factor 2.

Osteogenesis In Vivo

This study was conducted according to the protocol approved by the Animal Committee of Tokyo Medical and Dental University. Both maxillary and mandibular incisors were obtained from inbred Fisher 344 rats at 8 weeks old (Charles River) after sacrifice by carbon dioxide. Gingiva and dental pulp cells were prepared and cultured in osteogenic medium as described previously. Then the cell suspensions of 1×10^6 cells in 100 μl PBS were seeded into β-tricalcium phosphate (β-TCP) discs (porosity 75%, 5 mm diameter, 3 mm height, provided by HOYA, Tokyo, Japan) with 27-G needles. The discs were partially soaked with 5 ml osteogenic medium described above on 60-cm^2 culture dishes and incubated overnight at 37°C, under 5% CO^2 and saturated water vapor. β-TCP discs with 100 μl PBS only and without cells were served as controls. The discs were implanted in perivertebral muscles of rats under anesthesia with pentobarbital. After 6 weeks, β-TCP discs were removed and analyzed with a microCT ScanXmate-E090 system (Comscan) and Tri3D Bon (Ratoc System Engineering, Tokyo).

Statistics

Comparisons of total yields per tooth among gingiva, dental pulp, and periodontal ligament were performed using the Steel–Dwass multiple comparison test after the Kruskal–Wallis test. Comparisons of means between groups were performed using paired Student's *t*-test for the oil red O-positive colony rate, the alizarin red-positive colony rate, and quantitative PCR analysis. Differences at $p<0.05$ were considered significant.

RESULTS

Yields of Gingival, Dental Pulp, and Periodontal Ligament Cells

When cells were plated at a relatively low density (1×10^3 cells/60 cm^2; Fig. 1A), gingival cells and dental pulp cells formed a few colonies, but periodontal ligament cells formed no colonies (Fig. 1B). The colony number increased according to the number of nucleated cells plated. Gingival cells and dental pulp cells showed higher yield per tooth than periodontal ligament cells (Fig. 1C).

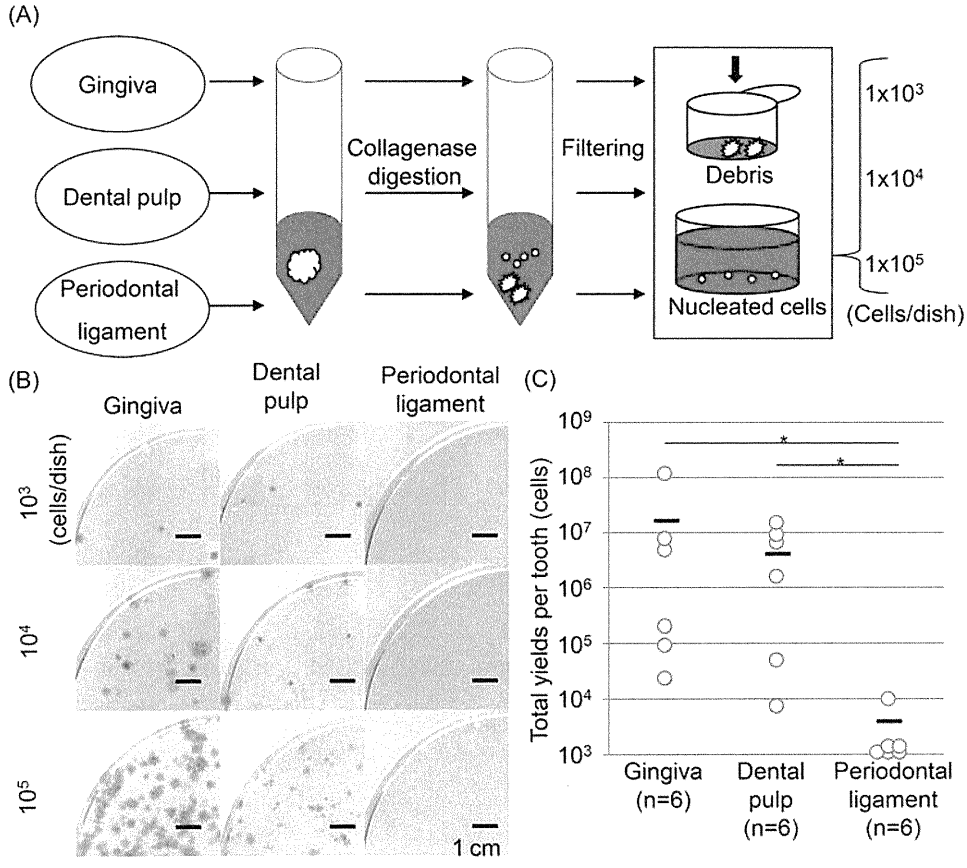

Figure 1. Properties of cells derived from gingiva, dental pulp, and periodontal ligament. (A) Preparation of cells. (B) Colony-forming ability. (C) Yields of cells derived from gingiva, dental pulp, and periodontal ligament cells per tooth after 14-day incubation ($n=6$, $p=0.004$ by the Kruskal–Wallis test and $*p<0.05$ by the Steel–Dwass multiple comparison test).

Yields of periodontal ligament cells were too low to perform further analysis.

Surface Epitopes

The positive rates for CD34, CD45, and CD117 were less than 3% on both gingival and dental pulp cells (Fig. 2). In contrast, the positive rates for CD44 were more than 97%, for CD90, CD105, and CD166 they were more than 60%, and for CD146 they were around 60%. There were no obvious differences of positive rates for surface epitopes we examined between gingival cells and dental pulp cells.

Chondrogenic Potential

After chondrogenic induction, the mRNA expression level of aggrecan, one of the chondrocyte-specific genes, increased significantly in both gingival and dental pulp cells (Fig. 3A). Both of these cells produced cartilage matrix positively stained with toluidine blue and immunostained with collagen type 2 (Fig. 3B). However, chondrogenic potentials of both gingival and dental pulp cells were inferior to those of synovial MSCs, which have a high chondrogenic potential by histological analyses (6,14).

Adipogenic Potential

After culturing in adipogenic medium, the mRNA expression level of adipsin, one of the adipocyte-specific genes, was increased significantly in both gingival and dental pulp cells (Fig. 4A). Though some colonies were stained with oil red O in both gingival and dental pulp cells, the number of colonies positive for oil red O was low (Figs. 4B and C). The oil red O-positive colony rate was higher in gingival cells (12.0%) than in dental pulp cells (2.4%) ($p<0.05$).

Osteogenic Potential In Vitro and In Vivo

The mRNA expression level of Runx2, an early marker for osteogenesis, was higher in dental pulp cells at 21 days than at 0 day (Fig. 5A). The mRNA expression level of osteocalcin, a late marker for osteogenesis, increased significantly in both gingival and dental pulp

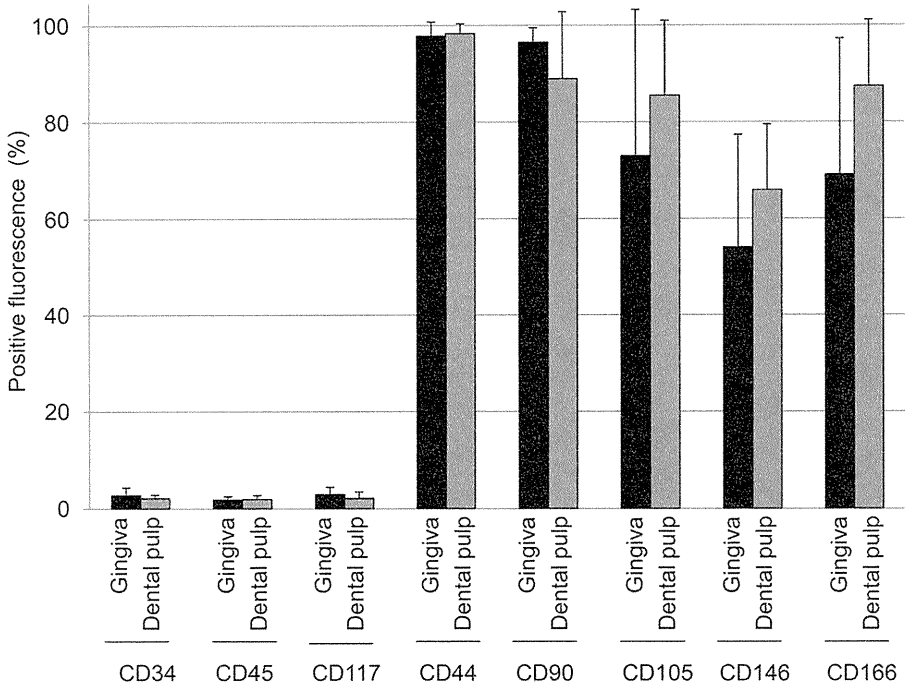

Figure 2. Expression of cell surface epitopes on gingival and dental pulp cells by flow cytometric analysis. Percentage positivity (%) is displayed as mean±standard deviation based on six donors.

cells after osteogenic induction. Approximately 60% of the colonies of gingival cells and 40% of the colonies of dental pulp cells were positively stained with alizarin red (Figs. 5B and C). The alizarin red-positive colony rate was higher in gingival cells than in dental pulp cells ($p<0.05$). Finally, in vivo osteogenic potentials of gingival and dental pulp cells were examined (Fig. 6A). At 6 weeks after implantation, the calcified area was larger in discs implanted with both gingival and dental pulp cells than in the control disc (Fig. 6B).

DISCUSSION

A considerable amount of retrospective data is available that describes putative MSCs; however, there is still

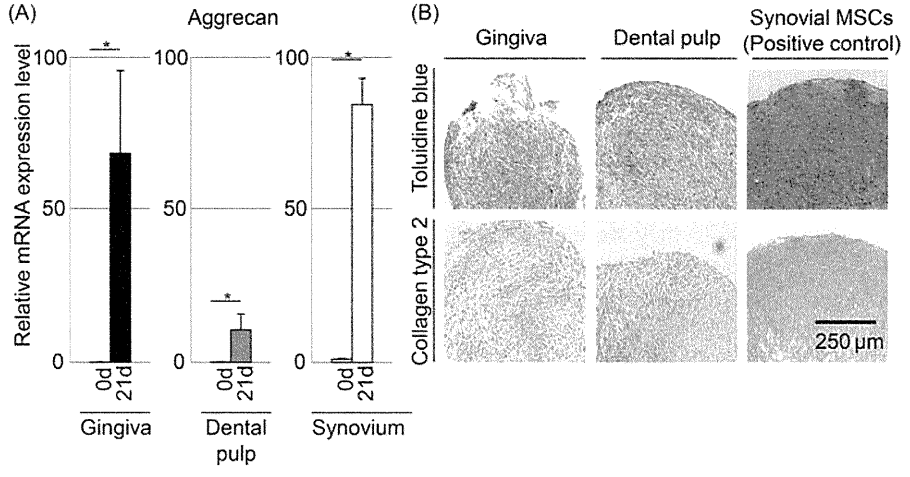

Figure 3. Chondrogenic potential of gingival and dental pulp cells. Synovial MSCs were used as a positive control. (A) Aggrecan mRNA expression by quantitative-PCR. The values are displayed as mean ± standard deviation of triplicates and are representative of three independent experiments ($n=3$ samples per group). *$p<0.05$ by paired Student's t test. (B) Histologies stained with toluidine blue and immunostained with collagen type 2.

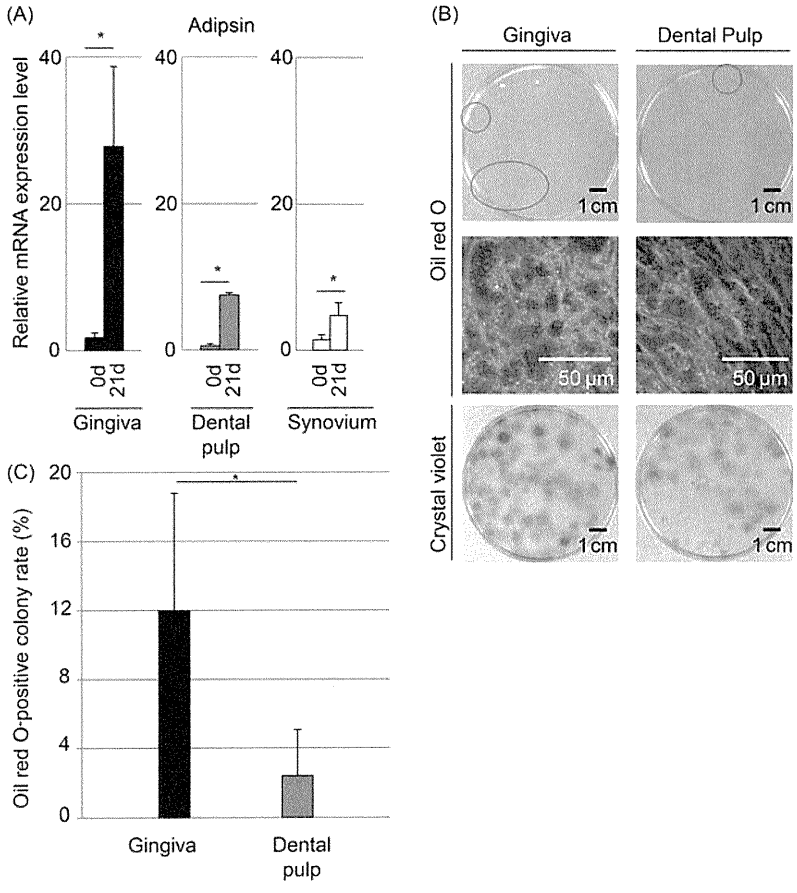

Figure 4. Adipogenic potential of gingival and dental pulp cells. (A) Adipsin mRNA expression by quantitative PCR. The values are displayed as mean±standard deviation of triplicates and are representative of three independent experiments ($n=3$ samples per group). *$p<0.05$ by paired Student's t test. (B) Colony-forming cells stained with oil red O and crystal violet. Oil red O-positive colonies are indicated with red circles at the top row. (C) Oil red O-positive colony rate. The values are displayed as mean±standard deviation ($n=3$). *$p<0.05$ by paired Student's t test.

very little knowledge available that documents the properties of MSCs, especially in their native environment. Although the precise identity of MSCs remains a challenge, we herein define an MSC as being derived from mesenchymal tissue and by its functional capacity both to self-renew and to generate a number of differentiated progeny (9). Since the earliest work by Friedenstein (3), the standard assay used to identify MSCs is the colony-forming unit fibroblast assay, which identifies adherent, spindle-shaped cells that proliferate to form colonies. By this method, we isolated colony-forming cells from gingiva and dental pulp. We also demonstrated the in vitro multipotentialities of these cells. Therefore, we referred to the cells from gingiva and dental pulp studied in this article as MSCs.

To compare properties of MSCs derived from gingiva, dental pulp, and periodontal ligament strictly, we used patient-matched samples to avoid donor variations. Also, we controlled initial cell density to avoid colony-to-colony contact inhibition because colony-to-colony contact inhibition affects proliferation potential, surface epitopes, and differentiation potential (16). The optimal initial cell density was 1×10^5 cells/60 cm^2 dish for gingiva and dental pulp cells according to the criteria described above. No remarkable contact inhibition was observed at this cell density. Furthermore, cells were compared at the same passage because differentiation potential decreases after every passage (24).

We first revealed that the yield of periodontal ligament cells per tooth was much lower than the yields of gingival and dental pulp MSCs. We could not harvest a sufficient number of periodontal ligament cells from a tooth after a 14-day culture in five donors among six donors to perform further analyses with periodontal ligament cells. Previously, several reports described MSCs derived from periodontal ligament (5,11,17). We suppose that only limited batches of periodontal ligament cells among a considerable number of samples were targeted for the

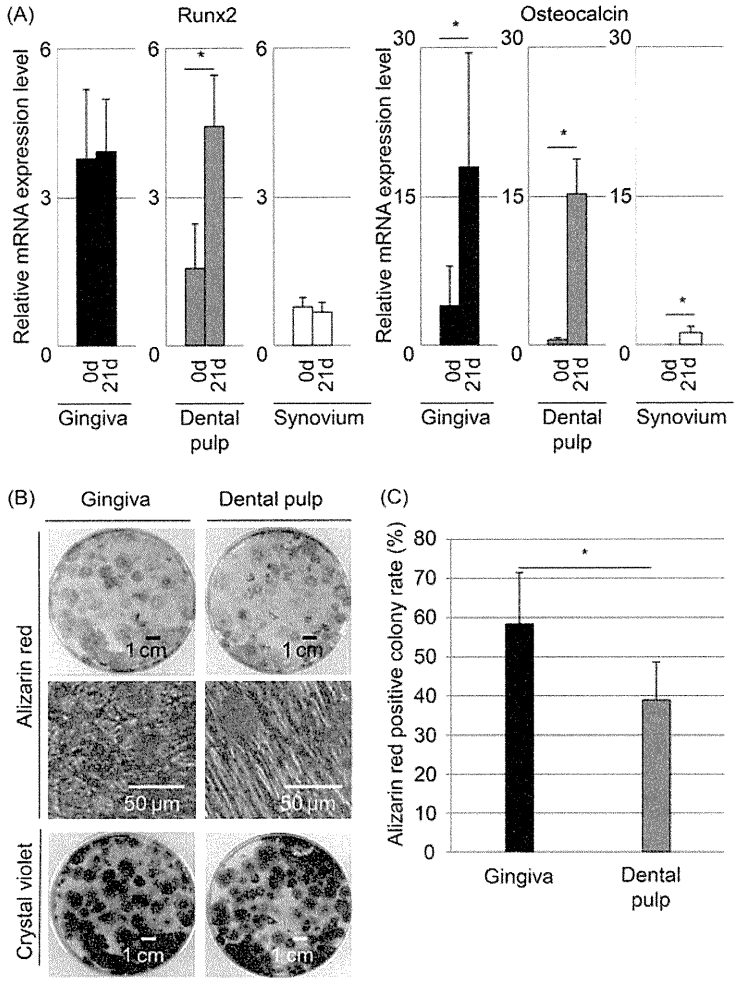

Figure 5. Osteogenic potential of gingival and dental pulp cells. (A) Runt-related transcription factor 2 (Runx2) and osteocalcin mRNA expression by quantitative PCR. The values are displayed as mean ± standard deviation of triplicates and are representative of three independent experiments ($n=3$ samples per group). *$p<0.05$ by paired Student's t test. (B) Colony-forming cells stained with alizarin red and crystal violet. (C) Alizarin red-positive colony rate. The values are displayed as mean ± standard deviation ($n=4$). *$p<0.05$ by paired Student's t test.

studies. In our opinion, periodontal ligament was not suitable as an MSC source for regenerative medicine because of low yields.

Epitope profiles of gingival MSCs and dental pulp MSCs were similar, in that the rate of positivity for CD34, CD45, and CD117 (hematopoietic stem cell markers) was low and the rate of positivity for CD44 (hyaluronan receptor), CD90 (Thy-1), CD105 (SH2), and CD166 (activated leukocyte cell adhesion molecule) was high. These results coincide with the phenotypic properties of bone marrow MSCs, synovial MSCs, and other MSCs (10,14,15). In this study, we examined only popular surface epitopes, and it would be intriguing to identify novel epitopes that are distinguished specifically among gingival, dental pulp, and other MSCs.

After chondrogenic induction, both gingival and dental pulp MSCs showed chondrogenic characteristics. However, histological analyses demonstrated that chondrogenic potentials of gingival and dental pulp MSCs were lower than those of synovial MSCs, which have high chondrogenic potential (6,14). This difference might have been due to the chondrogenic medium, for which the optimal combination of cytokines was determined by synovial MSCs (18).

After culturing in adipogenic medium, adipocyte-specific gene expression increased, and some colonies were stained with oil red O in both gingival and dental pulp MSCs. These findings indicate that both gingival and dental pulp MSCs had adipogenic potential. However, the oil red O-positive colony rate seemed to be extremely

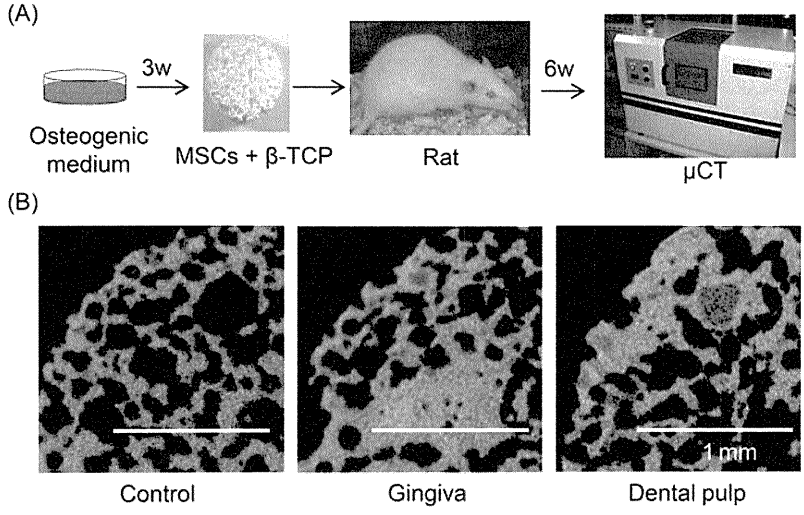

Figure 6. In vivo osteogenic potential of gingival and dental pulp cells after 6 weeks of implantation. (A) Protocol. (B) Microcomputed tomography images of implants.

lower in comparison to that of bone marrow MSCs and other MSCs reported previously (14), showing low adipogenic potential of gingival and dental pulp MSCs.

Osteogenesis-related genes increased in both gingival and dental pulp MSCs after osteogenic induction in vitro. The alizarin red-positive colony rate of both gingival and dental pulp MSCs was also comparable to those in other MSCs reported previously (14). Furthermore, both gingival and dental pulp MSCs increased the calcified area of the β-TCP disc after implantation into the muscle of rats. These results indicate that one of the characteristics of gingival and dental pulp MSCs is high osteogenic potential.

When we compare gingiva and dental pulp as a cell source for MSCs, gingiva is more appealing because of its easy accessibility. Gingiva can be harvested without removal of tooth. The high healing capability of gingiva at the donor site is also advantageous.

In this study, we demonstrated the usefulness of gingiva as a cell source for bone regeneration. Zhang et al. also reported the usefulness of gingiva as an MSC source, especially for its immunomodulatory effect in a mouse colitis model (25). However, Lin et al. negatively reported that gingival cells showed poor differentiational potential though they possessed proliferative efficiency to some extent (7). Other studies also reported lower osteogenic potential of gingival cells in comparison to that of periodontal ligament cells (19). The difference may be due to the procedure of preparation for gingival cell.

CONCLUSION

We clarified properties of MSCs derived from removed teeth. We were able to obtain a high yield of MSCs with osteogenic potential from gingiva and dental pulp. Our results indicate that gingiva and dental pulp are putative cell sources for hard tissue regeneration.

ACKNOWLEDGMENTS: We thank Miyoko Ojima for his expert help with histological analyses and Izumi Nakagawa for his help with laboratory management. This study was supported by "the Project for Realization of Regenerative Medicine" and "the Global Center of Excellence (GCOE) Program" by the Ministry of Education, Culture, Sports, Science and Technology (MEXT), Japan. Recombinant human bone morphogenetic protein-7 was kindly provided by Stryker Biotech. β-TCP discs were kindly provided by HOYA Corporation. The authors declare no conflicts of interest.

REFERENCES

1. Ballini, A.; De Frenza, G.; Cantore, S.; Papa, F.; Grano, M.; Mastrangelo, F.; Tete, S.; Grassi, F. R. In vitro stem cell cultures from human dental pulp and periodontal ligament: New prospects in dentistry. Int. J. Immunopathol. Pharmacol. 20:9–16; 2007.
2. De Bari, C.; Dell'accio, F. Mesenchymal stem cells in rheumatology: A regenerative approach to joint repair. Clin. Sci. 113:339–348; 2007.
3. Friedenstein, A. J. Precursor cells of mechanocytes. Int. Rev. Cytol. 47:327–359; 1976.
4. Gronthos, S.; Mankani, M.; Brahim, J.; Robey, P. G.; Shi, S. Postnatal human dental pulp stem cells (DPSCs) in vitro and in vivo. Proc. Natl. Acad. Sci. USA 97:13625–13630; 2000.
5. Gronthos, S.; Mrozik, K.; Shi, S.; Bartold, P. M. Ovine periodontal ligament stem cells: Isolation, characterization, and differentiation potential. Calcif. Tissue Int. 79: 310–317; 2006.
6. Koga, H.; Muneta, T.; Nagase, T.; Nimura, A.; Ju, Y. J.; Mochizuki, T.; Sekiya, I. Comparison of mesenchymal tissues-derived stem cells for in vivo chondrogenesis: Suitable conditions for cell therapy of cartilage defects in rabbit. Cell Tissue Res. 333:207–215; 2008.
7. Lin, N. H.; Menicanin, D.; Mrozik, K.; Gronthos, S.; Bartold, P. M. Putative stem cells in regenerating human periodontium. J. Periodontal Res. 43:514–523; 2008.

8. Marynka-Kalmani, K.; Treves, S.; Yafee, M.; Rachima, H.; Gafni, Y.; Cohen, M. A.; Pitaru, S. The lamina propria of adult human oral mucosa harbors a novel stem cell population. Stem Cells 28:984–995; 2010.
9. McKay, R. Stem cells in the central nervous system. Science 276:66–71; 1997.
10. Mochizuki, T.; Muneta, T.; Sakaguchi, Y.; Nimura, A.; Yokoyama, A.; Koga, H.; Sekiya, I. Higher chondrogenic potential of fibrous synovium- and adipose synovium-derived cells compared with subcutaneous fat-derived cells: Distinguishing properties of mesenchymal stem cells in humans. Arthritis Rheum. 54:843–853; 2006.
11. Nagatomo, K.; Komaki, M.; Sekiya, I.; Sakaguchi, Y.; Noguchi, K.; Oda, S.; Muneta, T.; Ishikawa, I. Stem cell properties of human periodontal ligament cells. J. Periodontal Res. 41:303–310; 2006.
12. Pierdomenico, L.; Bonsi, L.; Calvitti, M.; Rondelli, D.; Arpinati, M.; Chirumbolo, G.; Becchetti, E.; Marchionni, C.; Alviano, F.; Fossati, V.; Staffolani, N.; Franchina, M.; Grossi, A.; Bagnara, G. P. Multipotent mesenchymal stem cells with immunosuppressive activity can be easily isolated from dental pulp. Transplantation 80:836–842; 2005.
13. Sakaguchi, Y.; Sekiya, I.; Yagishita, K.; Ichinose, S.; Shinomiya, K.; Muneta, T. Suspended cells from trabecular bone by collagenase digestion become virtually identical to mesenchymal stem cells obtained from marrow aspirates. Blood 104:2728–2735; 2004.
14. Sakaguchi, Y.; Sekiya, I.; Yagishita, K.; Muneta, T. Comparison of human stem cells derived from various mesenchymal tissues: Superiority of synovium as a cell source. Arthritis Rheum. 52:2521–2529; 2005.
15. Segawa, Y.; Muneta, T.; Makino, H.; Nimura, A.; Mochizuki, T.; Ju, Y. J.; Ezura, Y.; Umezawa, A.; Sekiya, I. Mesenchymal stem cells derived from synovium, meniscus, anterior cruciate ligament, and articular chondrocytes share similar gene expression profiles. J. Orthop. Res. 27:435–441; 2009.
16. Sekiya, I.; Larson, B. L.; Smith, J. R.; Pochampally, R.; Cui, J. G.; Prockop, D. J. Expansion of human adult stem cells from bone marrow stroma: Conditions that maximize the yields of early progenitors and evaluate their quality. Stem Cells 20:530–541; 2002.
17. Seo, B. M.; Miura, M.; Gronthos, S.; Bartold, P. M.; Batouli, S.; Brahim, J.; Young, M.; Robey, P. G.; Wang, C. Y.; Shi, S. Investigation of multipotent postnatal stem cells from human periodontal ligament. Lancet 364:149–155; 2004.
18. Shirasawa, S.; Sekiya, I.; Sakaguchi, Y.; Yagishita, K.; Ichinose, S.; Muneta, T. In vitro chondrogenesis of human synovium–derived mesenchymal stem cells: Optimal condition and comparison with bone marrow-derived cells. J. Cell. Biochem. 97:84–97; 2006.
19. Somerman, M. J.; Archer, S. Y.; Imm, G. R.; Foster, R. A. A comparative study of human periodontal ligament cells and gingival fibroblasts in vitro. J. Dent. Res. 67:66–70; 1988.
20. Tang, L.; Li, N.; Xie, H.; Jin, Y. Characterization of mesenchymal stem cells from human normal and hyperplastic gingiva. J. Cell. Physiol. 226:832–842; 2011.
21. Tomar, G. B.; Srivastava, R. K.; Gupta, N.; Barhanpurkar, A. P.; Pote, S. T.; Jhaveri, H. M.; Mishra, G. C.; Wani, M. R. Human gingiva-derived mesenchymal stem cells are superior to bone marrow-derived mesenchymal stem cells for cell therapy in regenerative medicine. Biochem. Biophys. Res. Commun. 393:377–383; 2010.
22. Trubiani, O.; Scarano, A.; Orsini, G.; Di Iorio, D.; D'Arcangelo, C.; Piccirilli, M.; Sigismondo, M.; Caputi, S. The performance of human periodontal ligament mesenchymal stem cells on xenogenic biomaterials. Int. J. Immunopathol. Pharmacol. 20:87–91; 2007.
23. Uccelli, A.; Moretta, L.; Pistoia, V. Mesenchymal stem cells in health and disease. Nat. Rev. Immunol. 8:726–736; 2008.
24. Yoshimura, H.; Muneta, T.; Nimura, A.; Yokoyama, A.; Koga, H.; Sekiya, I. Comparison of rat mesenchymal stem cells derived from bone marrow, synovium, periosteum, adipose tissue, and muscle. Cell Tissue Res. 327:449–462; 2007.
25. Zhang, Q.; Shi, S.; Liu, Y.; Uyanne, J.; Shi, Y.; Le, A. D. Mesenchymal stem cells derived from human gingiva are capable of immunomodulatory functions and ameliorate inflammation-related tissue destruction in experimental colitis. J. Immunol. 183:7787–7798; 2009.

Implantation of Allogenic Synovial Stem Cells Promotes Meniscal Regeneration in a Rabbit Meniscal Defect Model

Masafumi Horie, MD, PhD, Matthew D. Driscoll, MD, H. Wayne Sampson, PhD, Ichiro Sekiya, MD, PhD, Cyrus T. Caroom, MD, Darwin J. Prockop, MD, PhD, and Darryl B. Thomas, MD

Investigation performed at Scott & White Memorial Hospital and the Texas A&M Health Science Center College of Medicine Institute for Regenerative Medicine, Temple, Texas

Background: Indications for surgical meniscal repair are limited, and failure rates remain high. Thus, new ways to augment repair and stimulate meniscal regeneration are needed. Mesenchymal stem cells are multipotent cells present in mature individuals and accessible from peripheral connective tissue sites, including synovium. The purpose of this study was to quantitatively evaluate the effect of implantation of synovial tissue-derived mesenchymal stem cells on meniscal regeneration in a rabbit model of partial meniscectomy.

Methods: Synovial mesenchymal stem cells were harvested from the knee of one New Zealand White rabbit, expanded in culture, and labeled with a fluorescent marker. A reproducible 1.5-mm cylindrical defect was created in the avascular portion of the anterior horn of the medial meniscus bilaterally in fifteen additional rabbits. Allogenic synovial mesenchymal stem cells suspended in phosphate-buffered saline solution were implanted into the right knees, and phosphate-buffered saline solution alone was placed in the left knees. Meniscal regeneration was evaluated histologically at four, twelve, and twenty-four weeks for (1) quantity and (2) quality (with use of an established three-component scoring system). A similar procedure was performed in four additional rabbits with use of green fluorescent protein-positive synovial mesenchymal stem cells for the purpose of tracking progeny following implantation.

Results: The quantity of regenerated tissue in the group that had implantation of synovial mesenchymal stem cells was greater at all end points, reaching significance at four and twelve weeks ($p < 0.05$). Tissue quality scores were also superior in knees treated with mesenchymal stem cells compared with controls at all end points, achieving significance at twelve and twenty-four weeks (3.8 versus 2.8 at four weeks [$p = 0.29$], 5.7 versus 1.7 at twelve weeks [$p = 0.008$], and 6.0 versus 3.9 at twenty-four weeks [$p = 0.021$]). Implanted cells adhered to meniscal defects and were observed in the regenerated tissue, where they differentiated into type-I and II collagen-expressing cells, at up to twenty-four weeks.

Conclusions: Synovial mesenchymal stem cells adhere to sites of meniscal injury, differentiate into cells resembling meniscal fibrochondrocytes, and enhance both quality and quantity of meniscal regeneration.

Clinical Relevance: These results may stimulate further exploration into the utility of synovial mesenchymal stem cells in the treatment of meniscal injury in large animals and humans.

The meniscus is a fibrocartilage structure functioning to increase surface contact area, absorb mechanical loads, and improve stability across the knee joint. Following injury, the human meniscus demonstrates poor healing potential because of the largely avascular nature of its fibrocartilaginous tissue. Failure rates after attempted surgical repair remain high, ranging from 24% to 50% for isolated meniscal tears[1-8]. As a result, partial meniscectomy is often the treatment of choice.

Disclosure: One or more of the authors received payments or services, either directly or indirectly (i.e., via his or her institution), from a third party in support of an aspect of this work. In addition, one or more of the authors, or his or her institution, has had a financial relationship, in the thirty-six months prior to submission of this work, with an entity in the biomedical arena that could be perceived to influence or have the potential to influence what is written in this work. No author has had any other relationships, or has engaged in any other activities, that could be perceived to influence or have the potential to influence what is written in this work. The complete **Disclosures of Potential Conflicts of Interest** submitted by authors are always provided with the online version of the article.

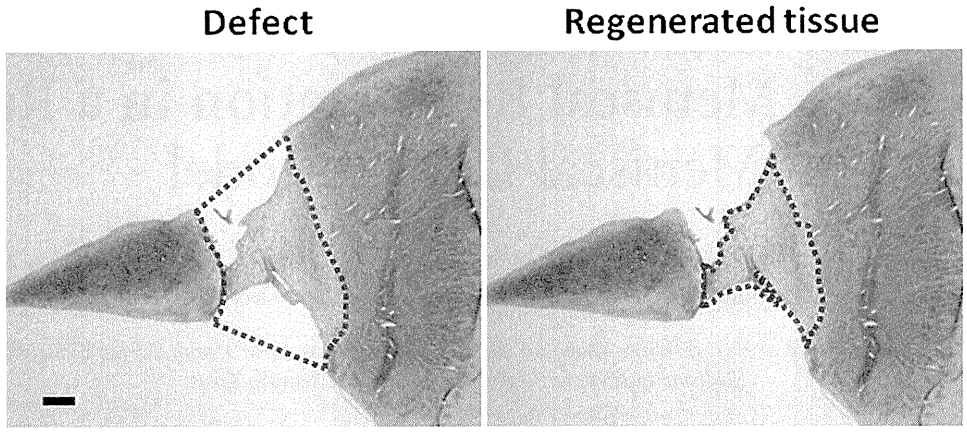

Fig. 1

Method of calculating the quantity of tissue regeneration. The area of the entire defect (D; blue dotted line; left) and the regenerated tissue (R; blue dotted line; right) were calculated. The regenerated tissue-to-defect ratio (R/D) was used to quantify the amount of regenerated meniscal tissue. The ideal quantity of regeneration would result in a value of 1, and incomplete regeneration would result in a value of <1. Scale bar represents 200 μm.

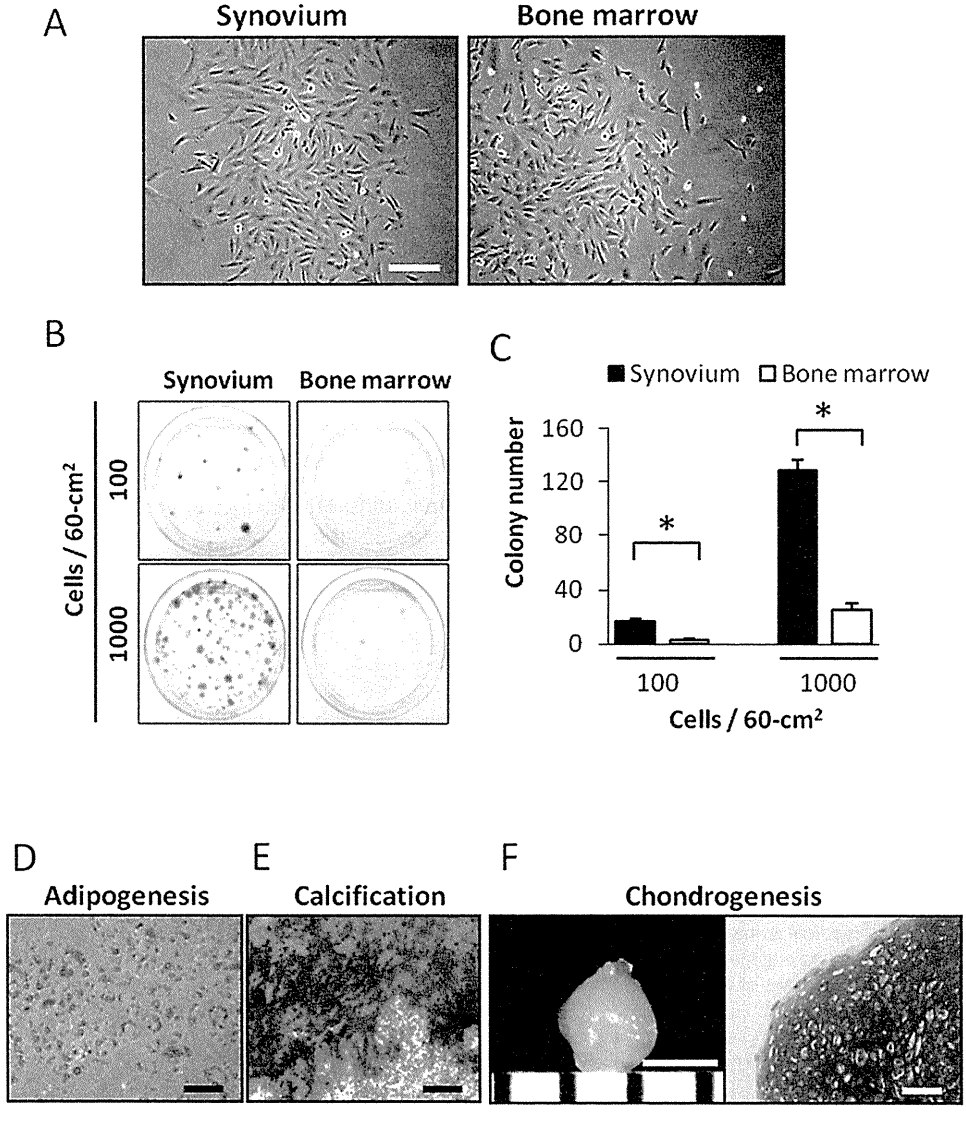

Fig. 2

Figs. 2-A through 2-F Synovial mesenchymal stem cells have high proliferation capacity and multipotentiality. *Synovium* refers to synovial mesenchymal stem cells, and *bone marrow* refers to bone-marrow mesenchymal stem cells. **Fig. 2-A** Histological appearance of synovial mesenchymal stem cells (left) and bone-marrow mesenchymal stem cells (right) at passage 3. Both groups formed monolayers of spindle-shaped cells that adhered to plastic culture dishes. Scale bar indicates 200 μm. **Fig. 2-B** Colony formation of synovial mesenchymal stem cells and bone-marrow mesenchymal stem cells at passage 3. Nucleated cells from synovium and bone marrow were plated at 100 and 1000 cells per 60-cm^2 dish and cultured for fourteen days (n = 5 cultures each). Culture dishes stained with crystal violet are shown. **Fig. 2-C** Graph showing the number of colonies (>2 mm) per dish at 100 or 1000 cells per 60 cm^2. *P < 0.01. **Fig. 2-D** Adipogenesis. Adipocyte colonies were stained with oil red O. Scale bar represents 200 μm. **Fig. 2-E** Calcification. Calcified colonies were stained with alizarin red. Scale bar represents 500 μm. **Fig. 2-F** Chondrogenesis. Gross photograph of a pellet (left). Scale bar represents 1 mm. Histological section of the pellet stained with safranin O (right). Scale bar represents 100 μm.

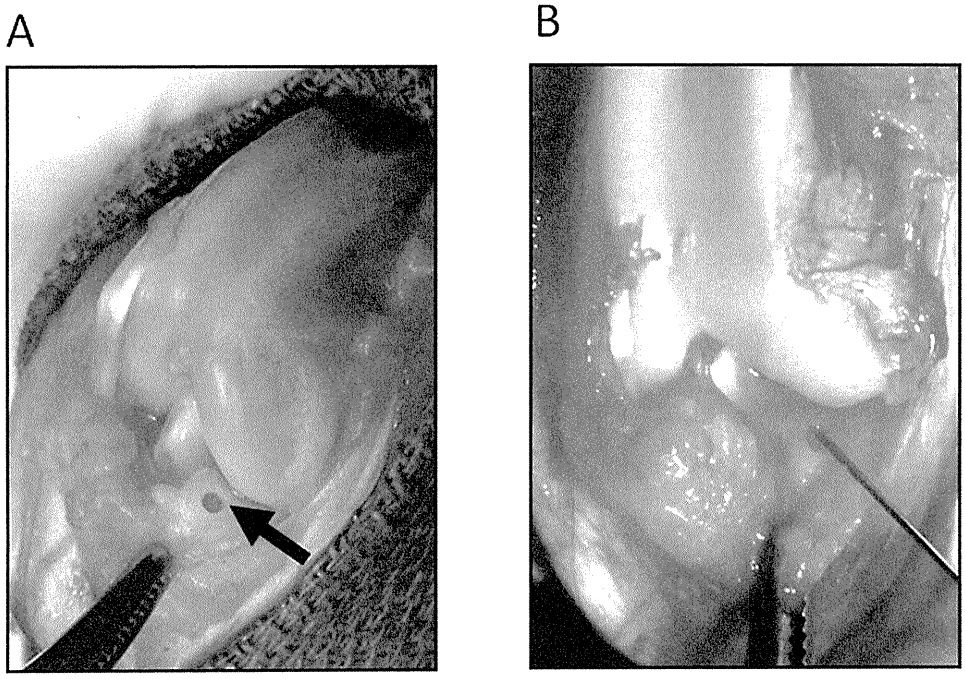

Fig. 3

Figs. 3-A and 3-B Meniscal biopsy and implantation of synovial mesenchymal stem cells. **Fig. 3-A** Intraoperative photograph made following meniscal biopsy. A 1.5-mm-diameter full-thickness cylindrical defect (arrow) was produced in the inner two-thirds of the anterior horn of the medial meniscus. **Fig. 3-B** Intraoperative photograph demonstrating implantation of the synovial mesenchymal stem cells. Two million synovial mesenchymal stem cells in 50 μL of phosphate-buffered saline solution were placed directly into the meniscal defect of experimental knees with use of a 27-gauge needle. In control knees, the same volume of plain phosphate-buffered saline solution was used.

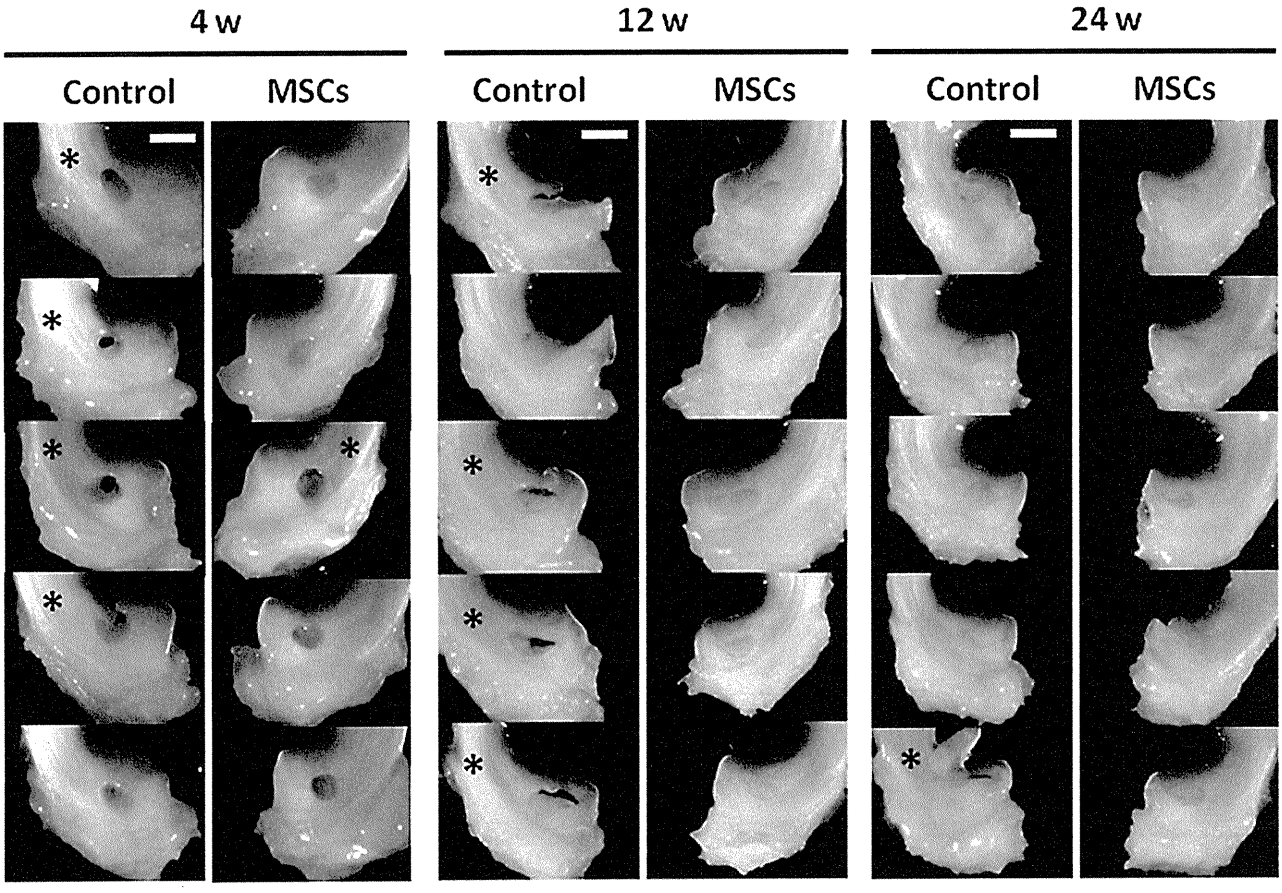

Fig. 4

Synovial mesenchymal stem cells (MSCs) promote meniscal regeneration (macroscopic observation). Macroscopic findings of the meniscus at four, twelve, and twenty-four weeks after the implantation of synovial mesenchymal stem cells. The specimens in which full-thickness grossly visible defects remained are denoted by an asterisk. Scale bar represents 2 mm.